Electronic supporting information

Multiplexed Fluorescent Polymeric Microstructures Sequentially Encoded via Two-Photon Click Tetrazole-based Chemistry.

Rana Mhanna[1], Nicolas Fournier Le Ray[2], Stephania Abdallah[1], Aissa Id Boualim[1], Jean-Luc Fillaut[2], Jean-Pierre Malval*[1].

[1] Institut de Science des Matériaux de Mulhouse CNRS-UMR 7361, Université de Haute Alsace, 15 rue Jean Starcky, 68057, Mulhouse, France.

[2] Université Rennes, Institut des Sciences Chimiques de Rennes CNRS UMR 6225, F-35000 Rennes.

E-Mails: jean-pierre.malval@uha.fr

CONTENTS

1. Figures and Tables.

2. Synthesis of tetrazoles derivatives.

3. Materials and General Characterization Methods.

4. References

1. Figures and Tables.

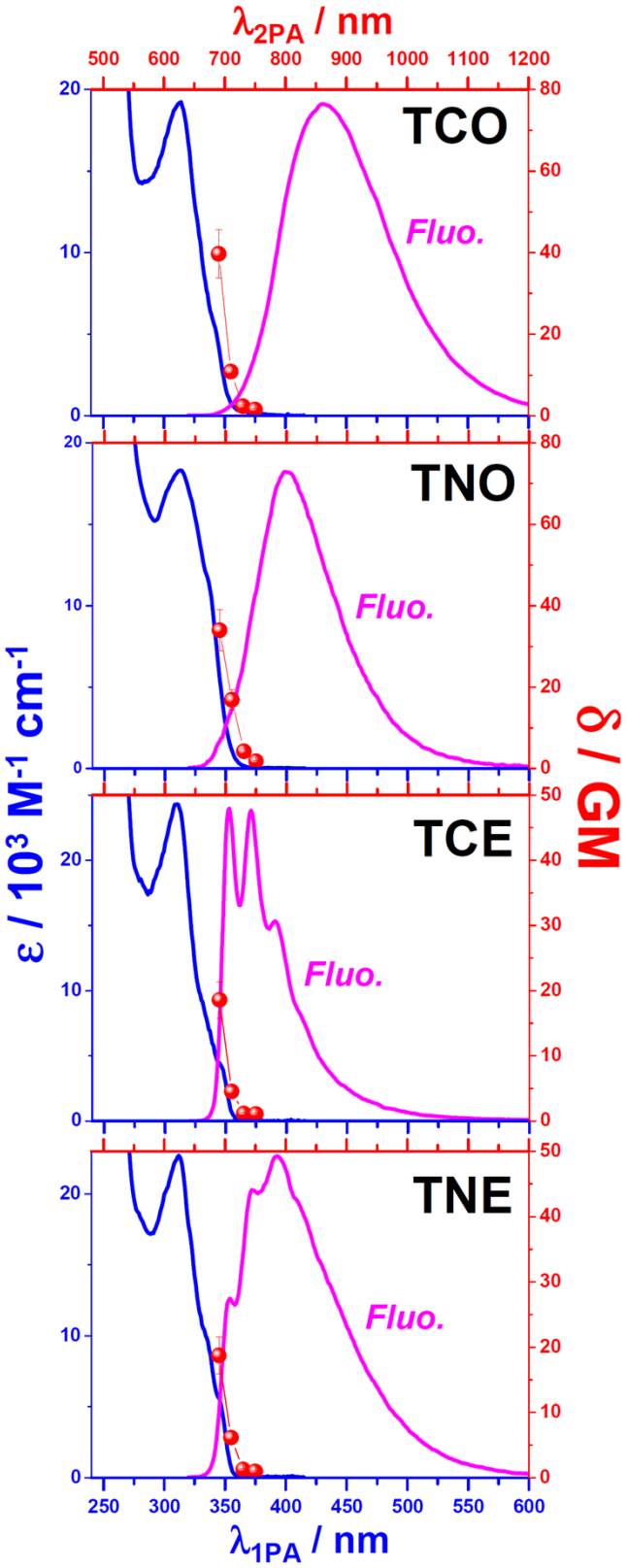

Figure S1. One- (blue line) and two-photon (circles) absorption spectra of tetrazoles in ACN. The fluorescence spectrum of each dye in ACN is also added.

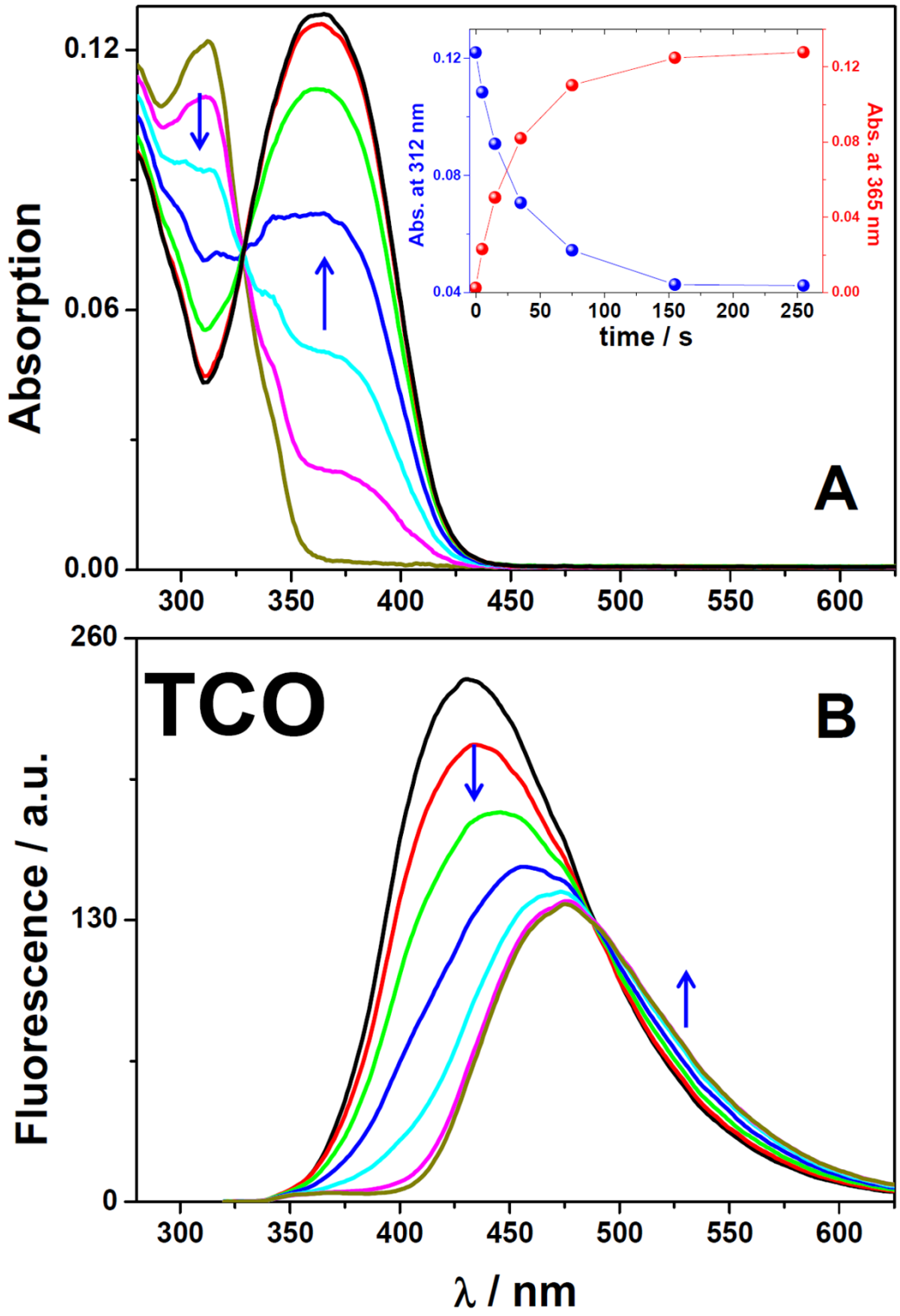

Figure S2. Evolution of the absorption (A) and fluorescence (B) spectra of **TCO** (6.2 μM) in presence of **PETIA** monomer (10 eq.) during irradiation at 315 nm in ACN. Inset in A: Time courses of the absorbances at 312 nm and 365 nm.

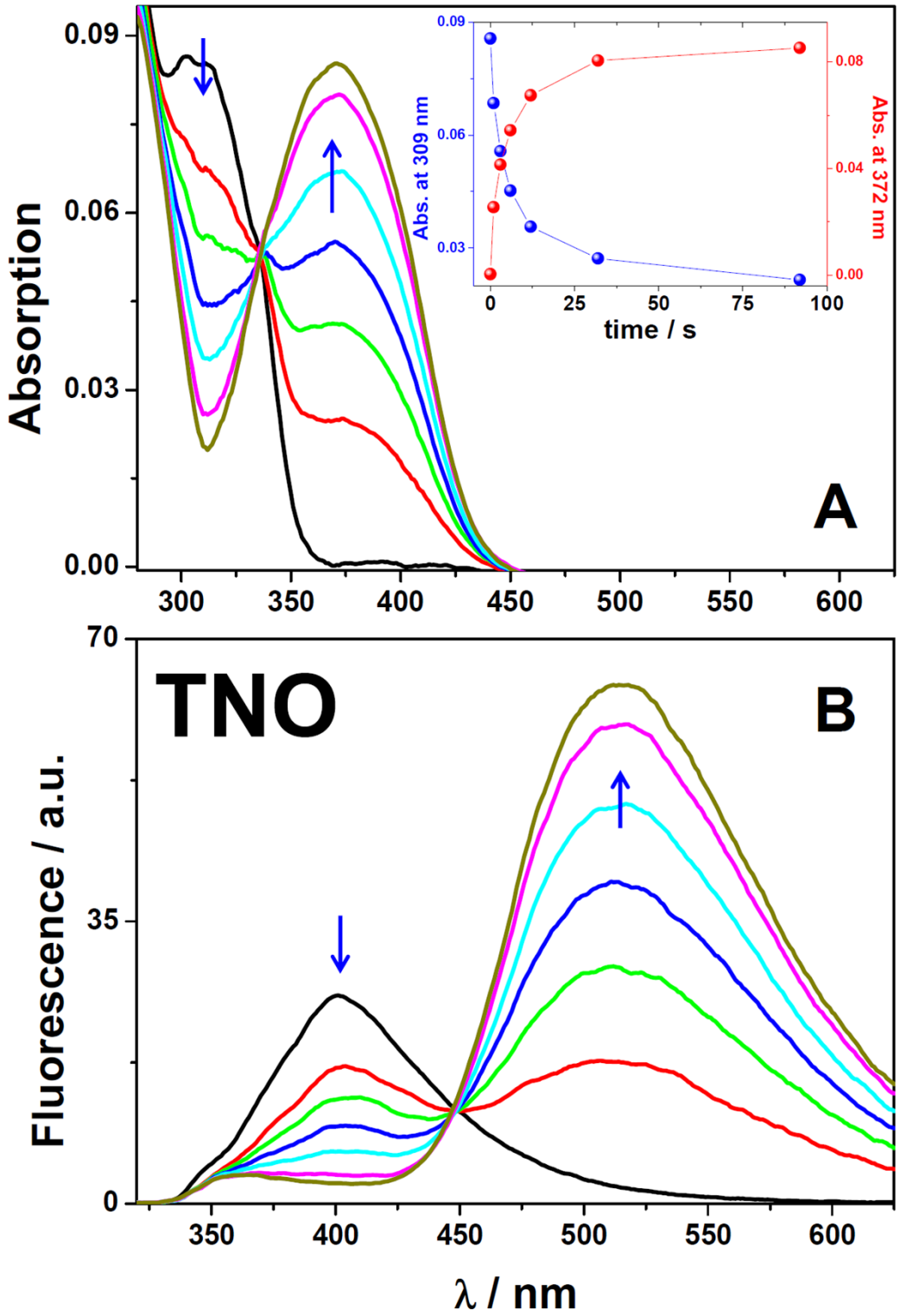

Figure S3. Evolution of the absorption (A) and fluorescence (B) spectra of **TNO** (4.7 μM) in presence of **PETIA** monomer (10 eq.) during irradiation at 315 nm in ACN. Inset in A: Time courses of the absorbances at 309 nm and 372 nm.

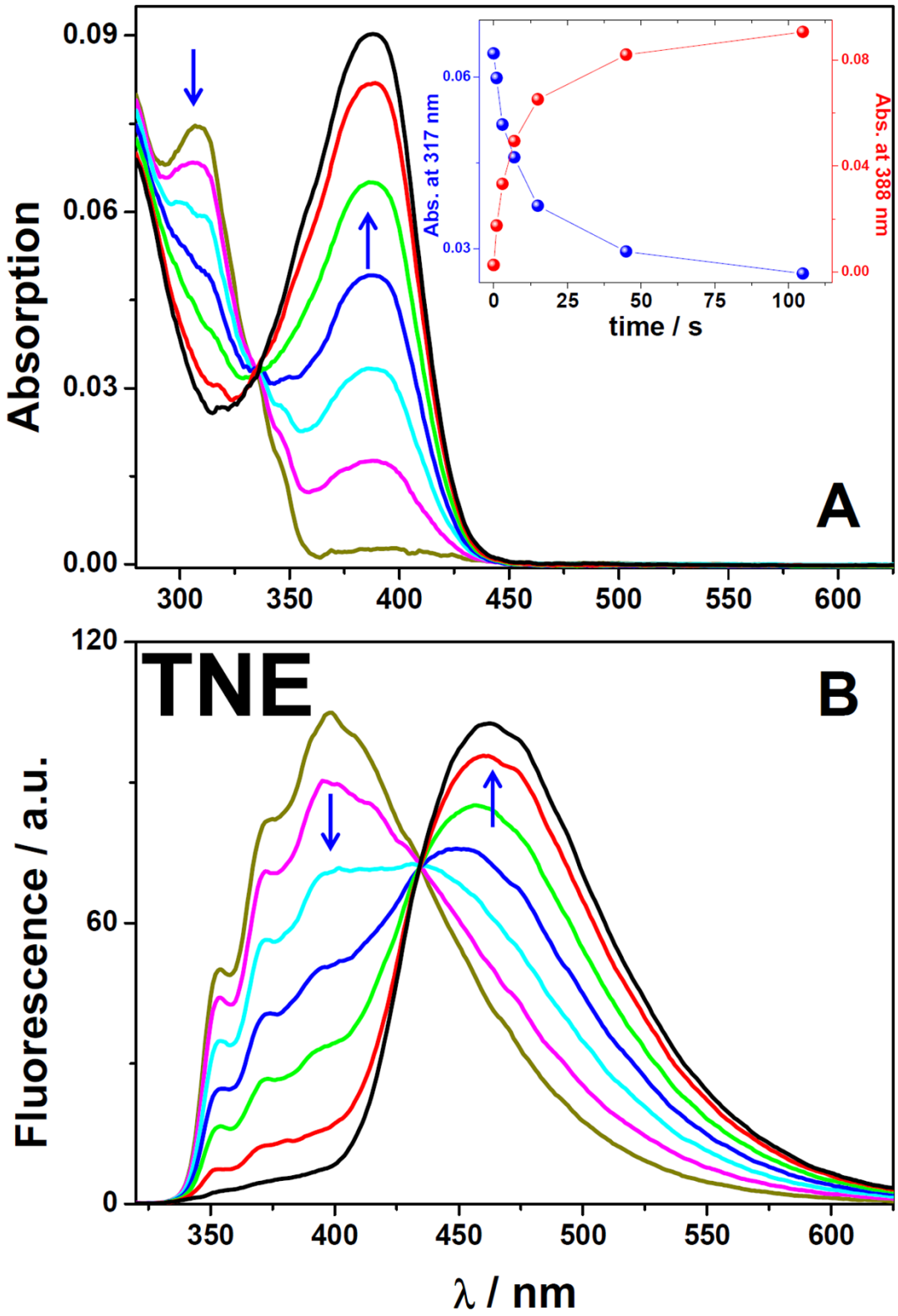

Figure S4. Evolution of the absorption (A) and fluorescence (B) spectra of **TNE** (3.3 μM) in presence of **PETIA** monomer (10 eq.) during irradiation at 315 nm in ACN. Inset in A: Time courses of the absorbances at 317 nm and 388 nm.

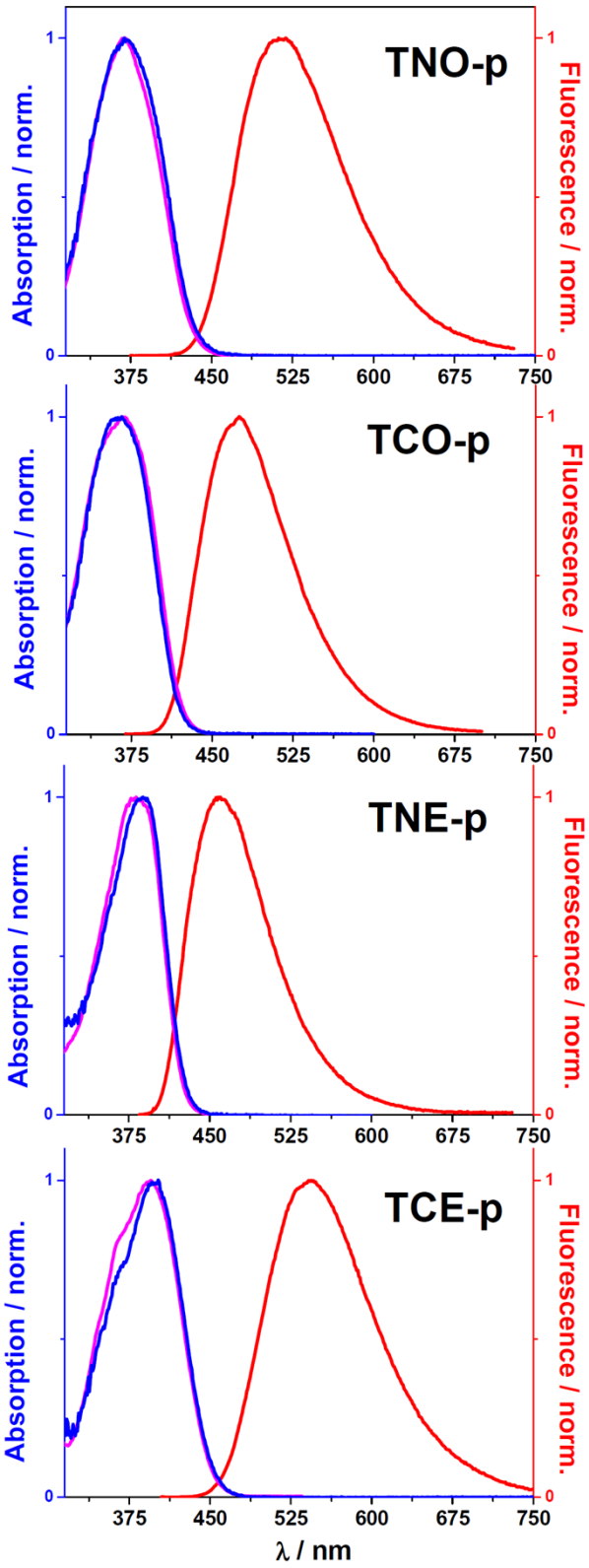

Figure S5. Normalized absorption (blue lines) and fluorescence (red lines) spectra of pyrazoline cycloadducts in ACN. The excitation spectrum of each compound (magenta line) has been also superimposed with the corresponding absorption spectrum.

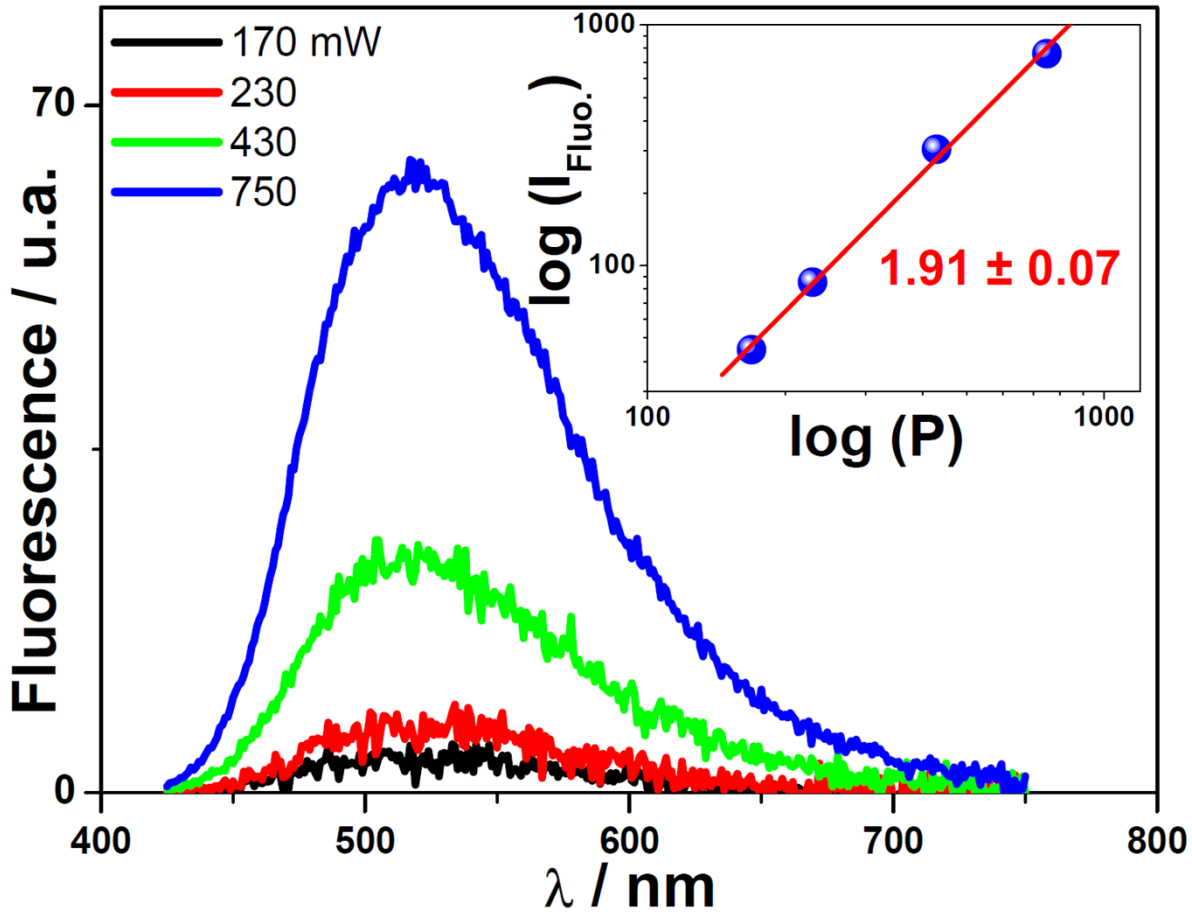

Figure S6. Fluorescence spectra monitoring of the cycloaddition reaction of **TNO** (0.15 mM) and **PETIA** (10 eq.) in ACN under *fs*-pulsed laser irradiation at 700 nm for different excitation powers. Inset: Quadratic dependence of the integrated fluorescence signal *vs.* incident power at 700 nm

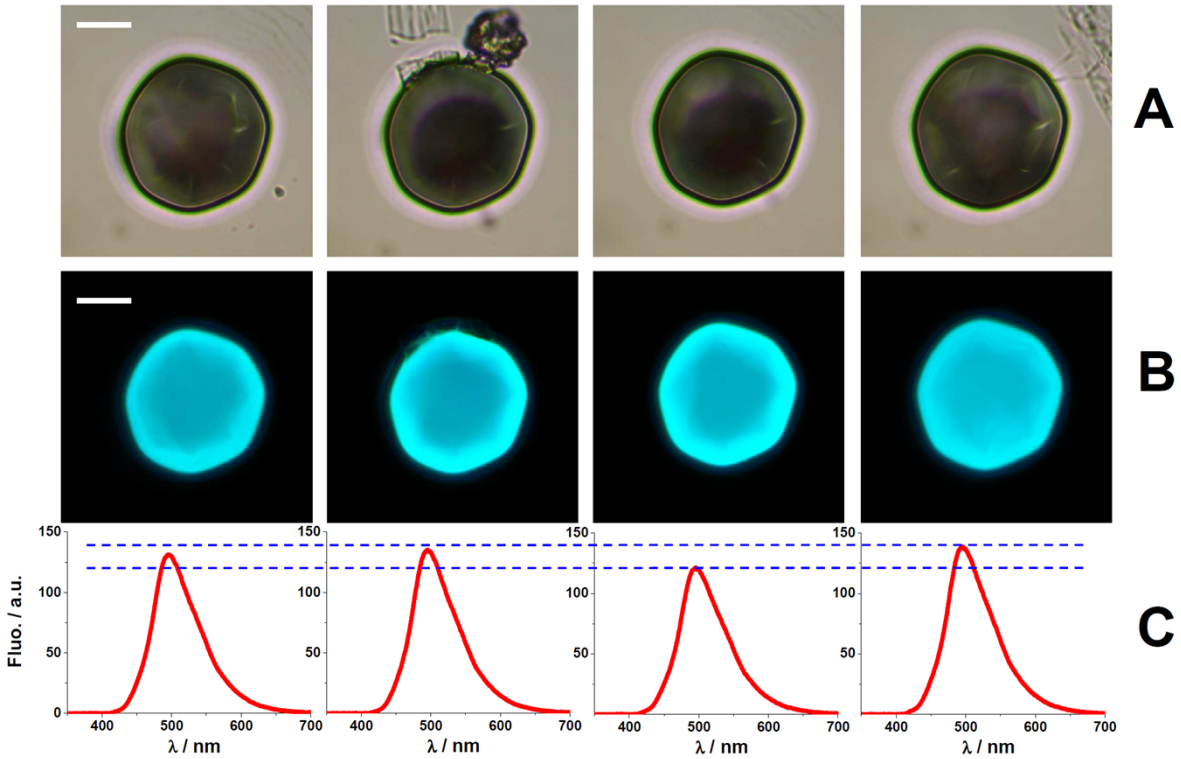

Figure S7. Example of four polyacrylate µ-dots functionalized with **TCE**-based pyrazolines after photoclick reactions at 365 nm. **A.** Transmitted optical images of the µ-dots in air (scale bar: 20 µm). **B.** Epiluminescence images from the µ-dots upon excitation at 365 nm (scale bar: 20 µm). **C.** Epifluorescence spectra recorded from the corresponding µ-dots. Note that the fluorescence spectra are not corrected and are truncated in their blue region due to the dichroic mirror response and the long pass filter necessary for the excitation cut-off. The horizontal dashed lines denote the variation of the fluorescence maximum intensity between the four spectra leading to an uncertainty of about 8 %.

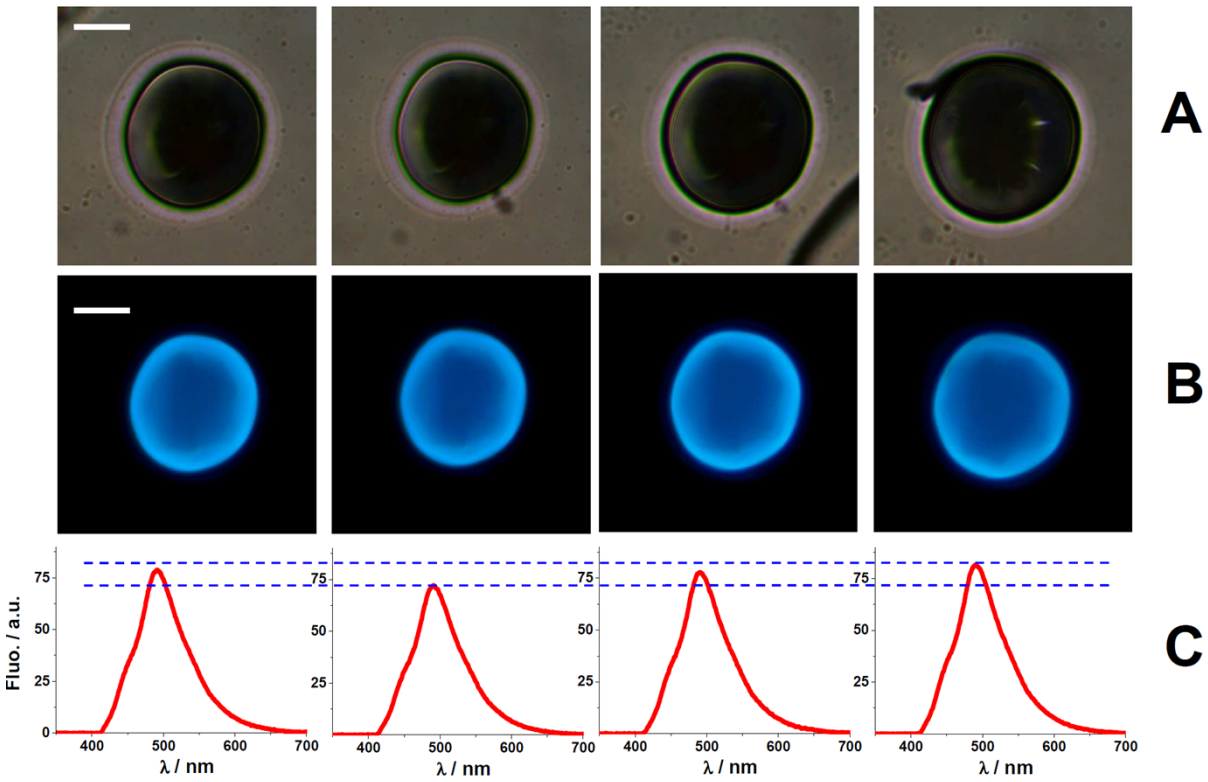

Figure S8. Example of four polyacrylate µ-dots functionalized with **TNO**-based pyrazolines after photoclick reactions at 365 nm. **A.** Transmitted optical images of the µ-dots in air (scale bar: 20 µm). **B.** Epiluminescence images from the µ-dots upon excitation at 365 nm (scale bar: 20 µm). **C.** Epifluorescence spectra recorded from the corresponding µ-dots. Note that the fluorescence spectra are not corrected and are truncated in their blue region due to the dichroic mirror response and the long pass filter necessary for the excitation cut-off. The horizontal dashed lines denote the variation of the fluorescence maximum intensity between the four spectra leading to an uncertainty of about 8 %

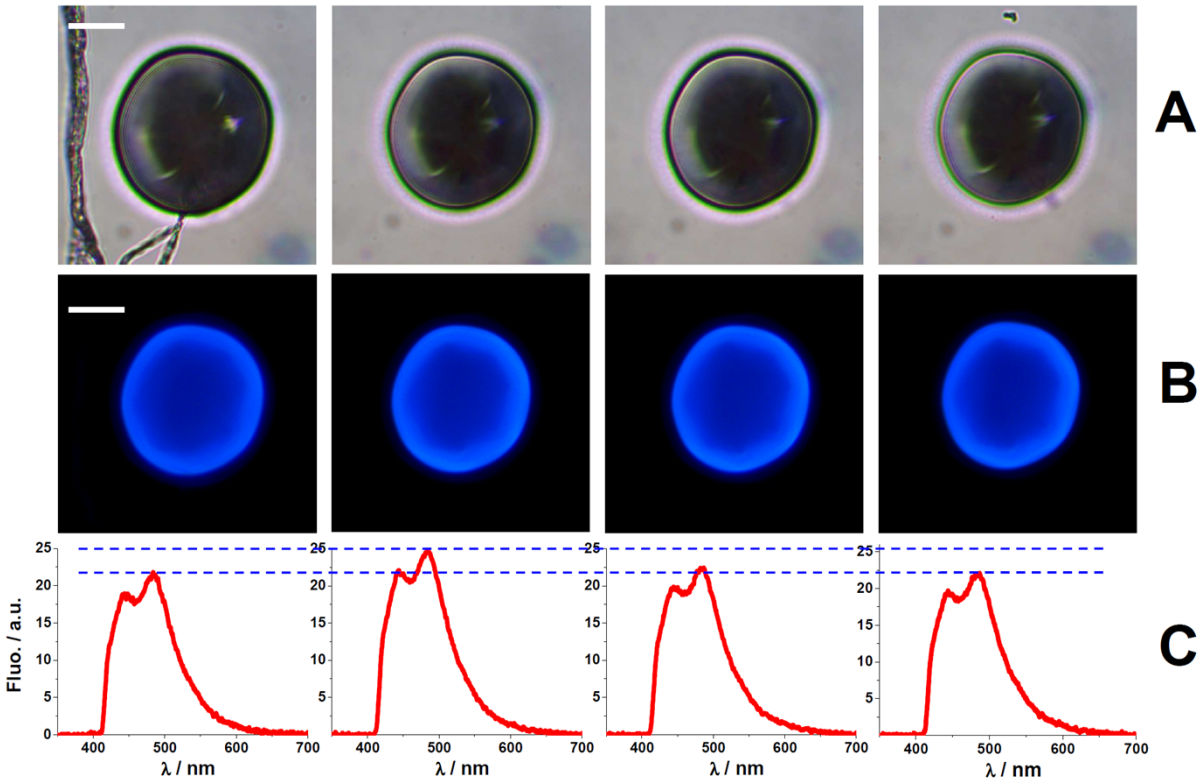

Figure S9. Example of four polyacrylate µ-dots functionalized with **TCO**-based pyrazolines after photoclick reactions at 365 nm. **A.** Transmitted optical images of the µ-dots in air (scale bar: 20 µm). **B.** Epiluminescence images from the µ-dots upon excitation at 365 nm (scale bar: 20 µm). **C.** Epifluorescence spectra recorded from the corresponding µ-dots. Note that the fluorescence spectra are not corrected and are truncated in their blue region due to the dichroic mirror response and the long pass filter necessary for the excitation cut-off. The horizontal dashed lines denote the variation of the fluorescence maximum intensity between the four spectra leading to an uncertainty of about 7 %

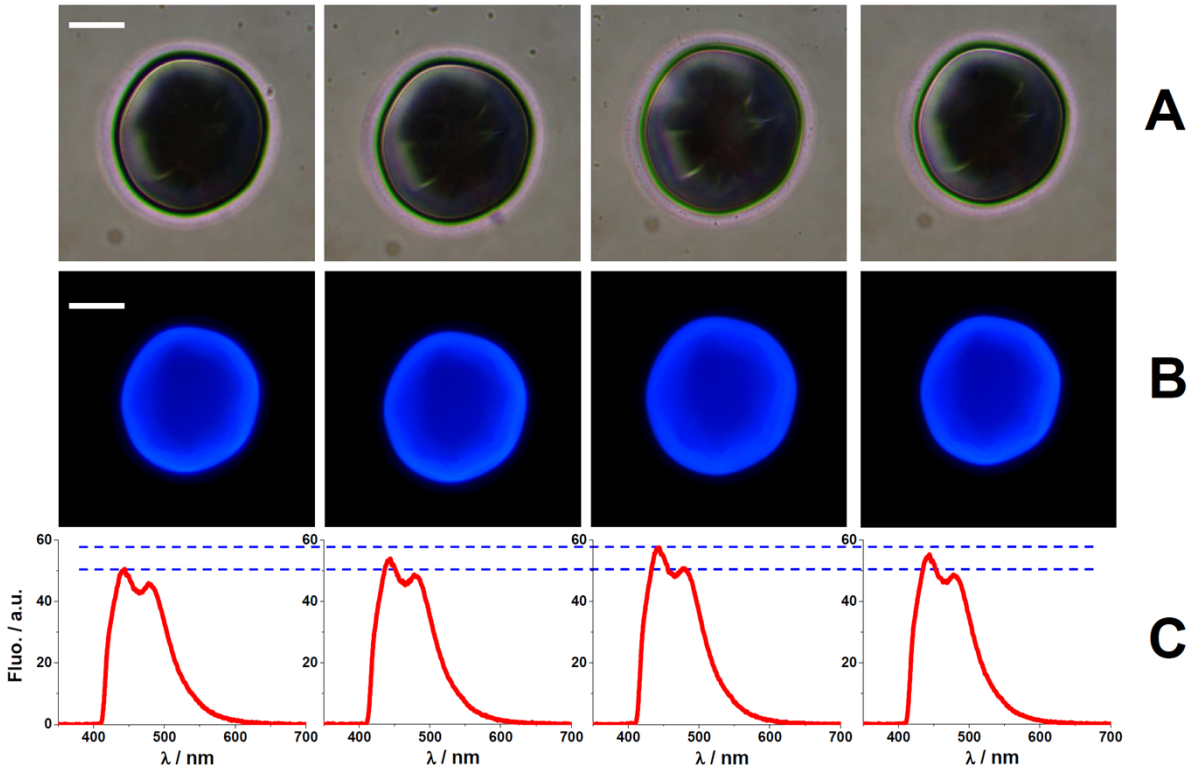

Figure S10. Example of four polyacrylate µ-dots functionalized with **TNE**-based pyrazolines after photoclick reactions at 365 nm. **A.** Transmitted optical images of the µ-dots in air (scale bar: 20 µm). **B.** Epiluminescence images from the µ-dots upon excitation at 365 nm (scale bar: 20 µm). **C.** Epifluorescence spectra recorded from the corresponding µ-dots. Note that the fluorescence spectra are not corrected and are truncated in their blue region due to the dichroic mirror response and the long pass filter necessary for the excitation cut-off. The horizontal dashed lines denote the variation of the fluorescence maximum intensity between the four spectra leading to an uncertainty of about 7 %

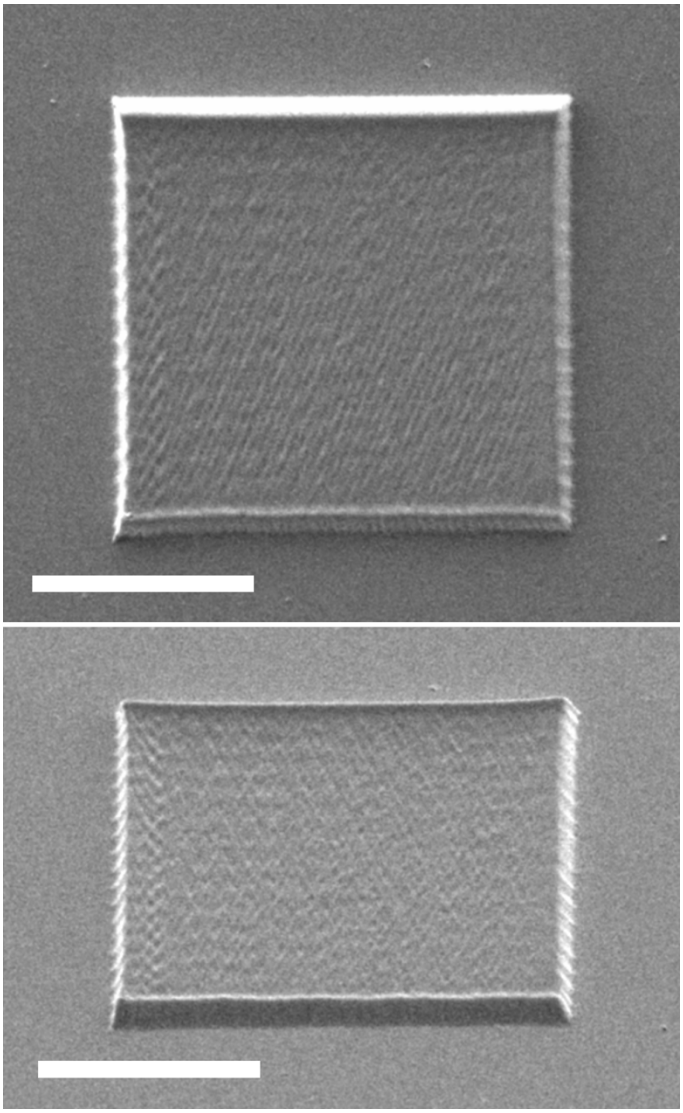

Figure S11. SEM images of a two-photon polymerized square shaped μ-slab. The SEM image at the bottom was recorded with a tilt angle of 45° (scale bar : 10 μm)

	λ_{abs} / nm	λ_{fluo} / nm	Φ_{fluo}
TCO-p	368	456	0.61
TNO-p	371	489	0.65
TCE-p	397	508	0.73
TNE-p	384	448	0.71

Table S1. Spectrocopic properties of pyrazoline cycloadducts in ACN .

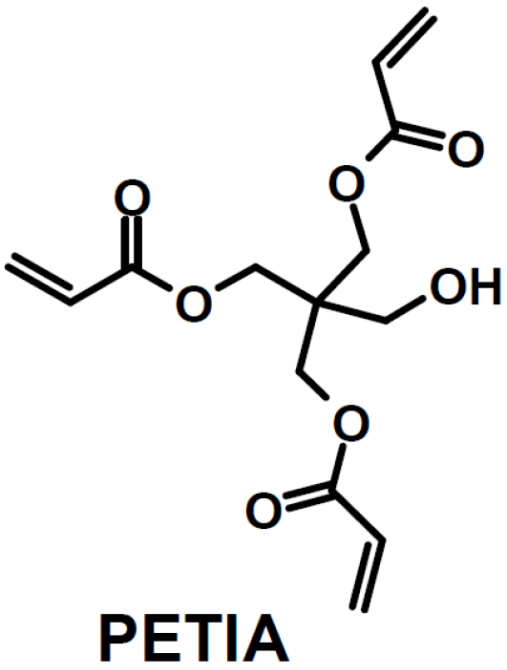

Scheme S1. Molecular structure of **PETIA** monomer.

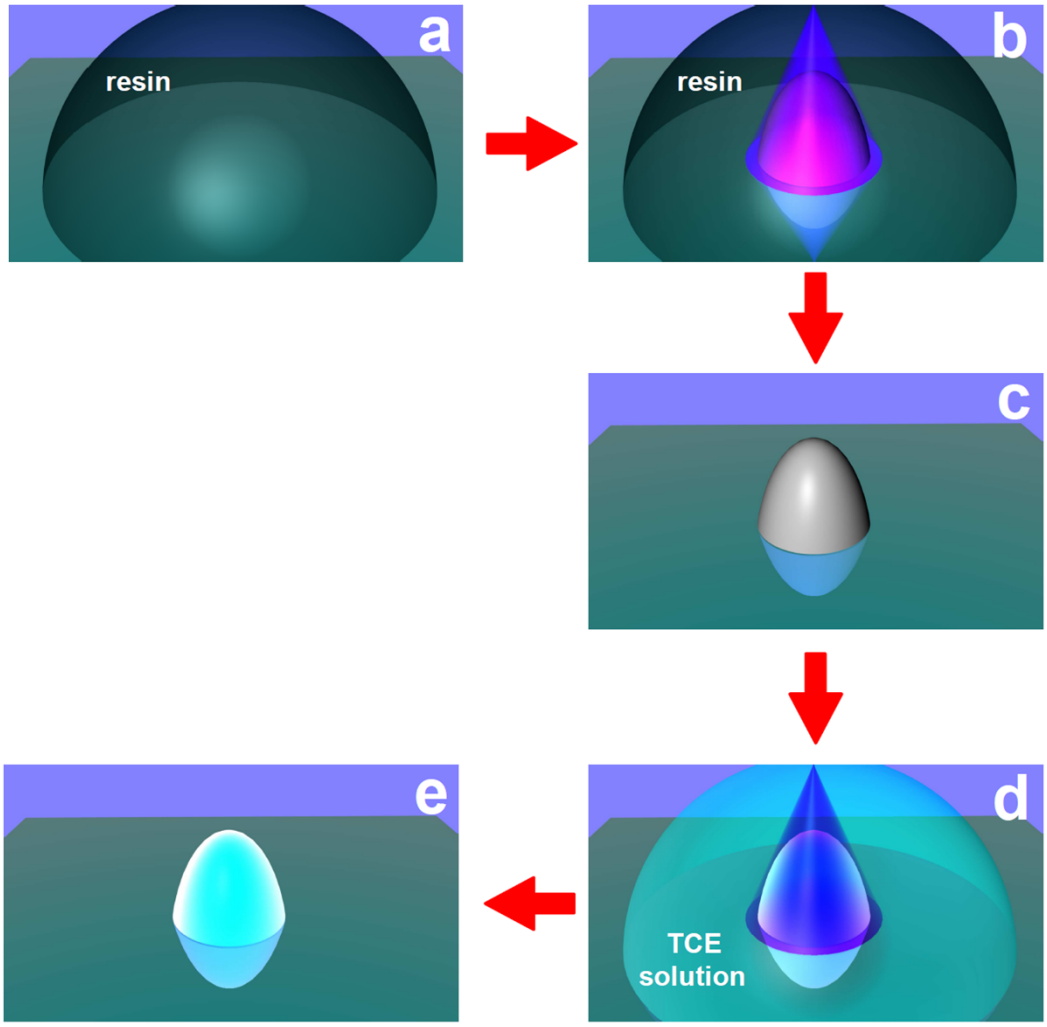

Scheme S2. Representative scheme for one-photon click labeling of a polymer dot: (a) Deposition of a drop a the triacrylate resin (**PETIA** with **TPO-L** / 4 wt%) on a glass coverslip. (b) In situ generation of photopolymerized dot through a 40X, 0.65-NA objective at 365 nm ($P_{365\ nm}$ = 1 µW, Δt = 2s). (c) Rinsing step with ethanol (d) In situ photoinduced labeling of the polymer dot immersed in a **TCE** acetonitrile solution (0.15 mM) (e) Rinsing step with chloroform then ethanol.

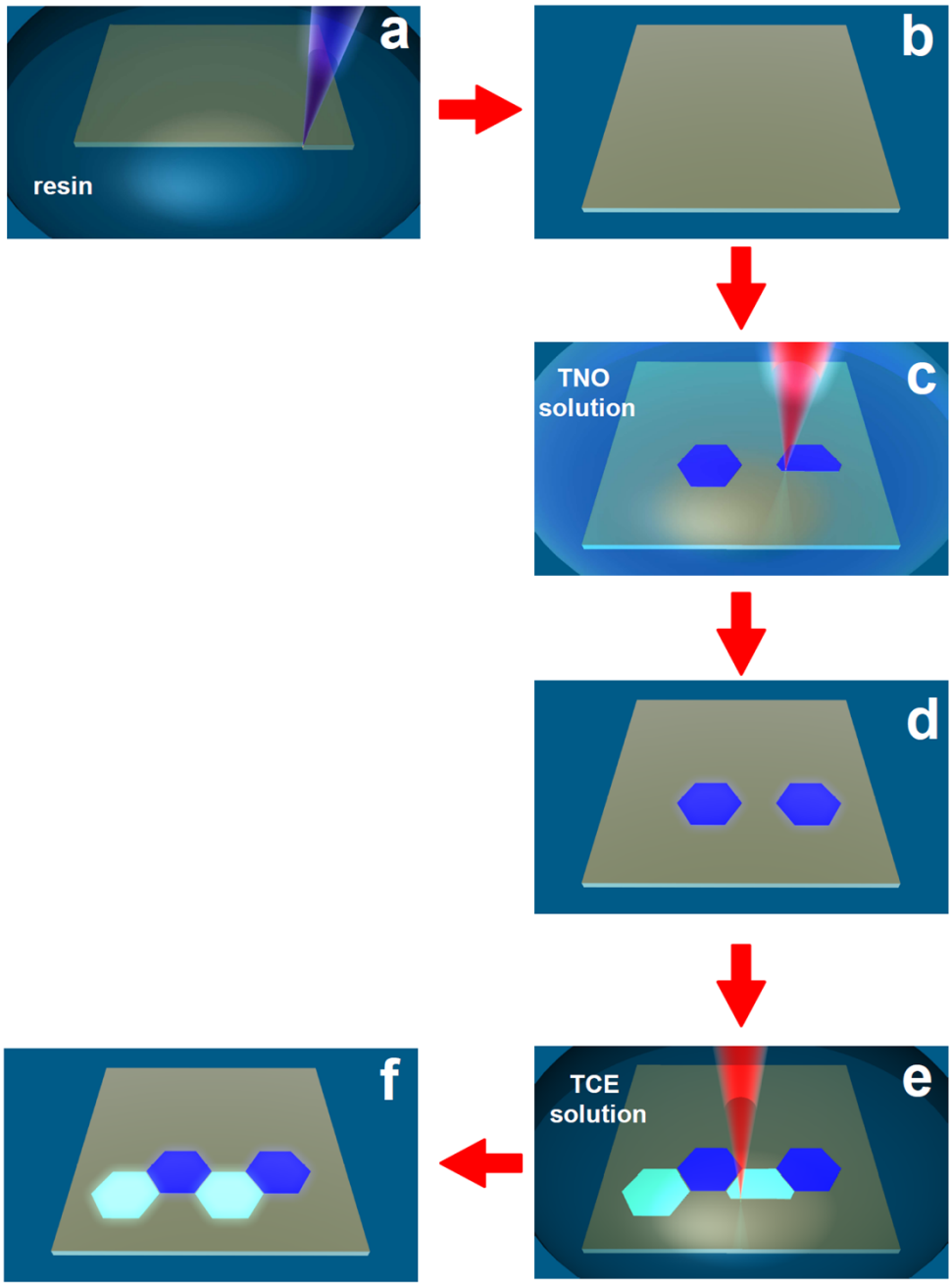

Scheme S3. Representative scheme for two-photon click labeling of a polymer µ-slab based on two functionalization sequences using successively **TNO** then **TCE** : (a) Two-photon fabrication of a polyacrylate µ-slab at 800 nm. (b) Rinsing step with ethanol. (c) In situ two-photon labeling of the µ-slab immersed in a **TNO** acetonitrile solution (c = 0.15 mM, $\lambda_{irr.}$ = 700 nm). (d) Rinsing step with chloroform then ethanol. (e) In situ two-photon labeling of the µ-slab immersed in a **TCE** acetonitrile solution (c = 0.15 mM, $\lambda_{irr.}$ = 700 nm). (f) Rinsing step with chloroform then ethanol.

2. Synthesis of tetrazoles derivatives.

All solvents were dried and purified by standard procedures. The syntheses were performed under an argon atmosphere. NMR spectra were recorded on Bruker DPX-200, AV 300 or AV 500 MHz spectrometers. ^{1}H and ^{13}C chemical shifts are given versus $SiMe_4$ and were determined by reference to residual ^{1}H and ^{13}C solvent signals. Mass spectrometric measurements have been made on a MAXIS 4G (Method ASAP) at the Centre de Mesures Physiques de l'Ouest (CRMPO) in Rennes.

The general synthetic route for the production of the tetrazoles derivatives is depicted in the following scheme[1]:

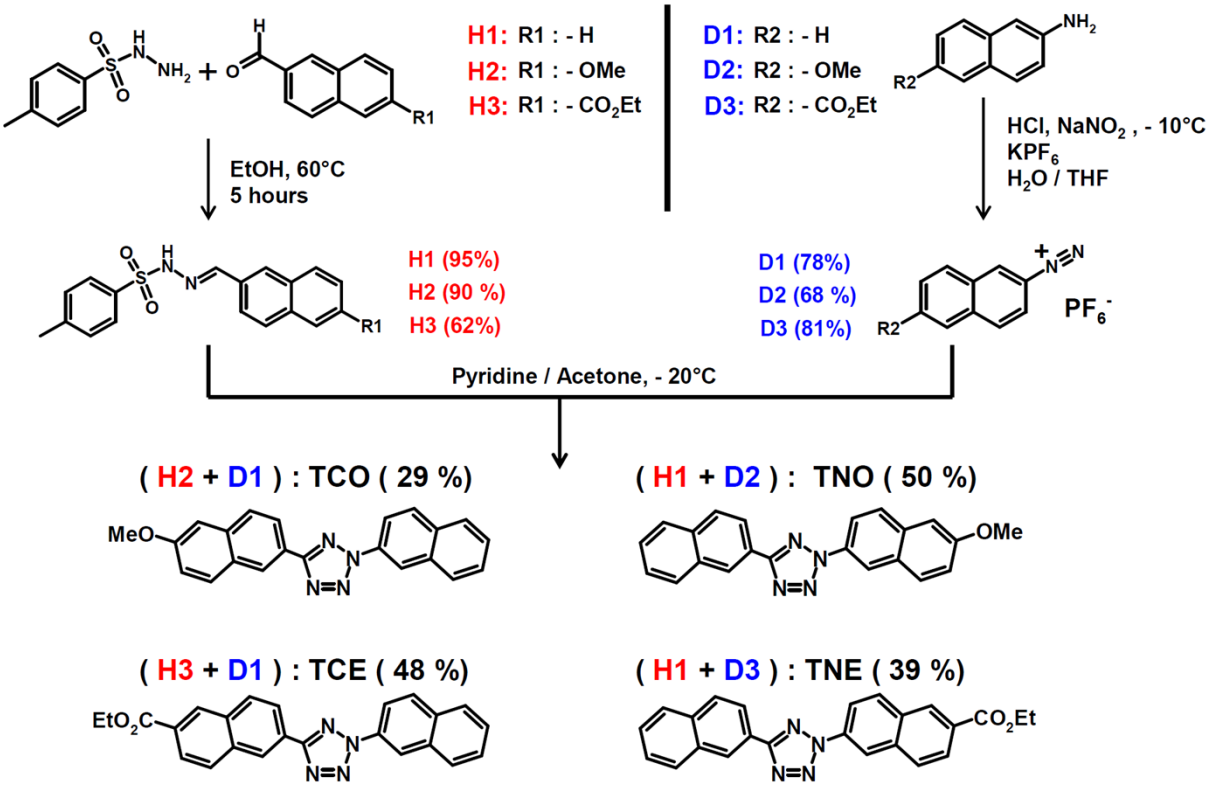

The sulfonyl hydrazones **H1-3** have obtained using p-toluenesulfonyl hydrazide (1eq. see the weights below) in 15 ml EtOH and heated at 60°C. The appropriate naphthalene-based aldehyde (1 eq., see the weights below) is then added to the solution leading to the rapid formation of a precipitate. After five hours heating, the reaction mixture was cooled to ambient temperature. The filtered the precipitate is successively washed with 20 ml of heptane and 20 ml of pentane then dried under vacuum yielding the corresponding p-toluenesulfonyl hydrazones. Note that all the aldehydes reactants are commercially

available except the ethyl 6-formylnaphthalene-2-carboxylate which was synthesized as described in reference[1].

H1 product is obtained using p-toluenesulfonyl hydrazide (1.79 g, 9.6 mmol) and 2-naphthaldehyde (1.51g, 9.6 mmol) which leads to a white powder (2.96 g, 95 %).
^{1}H NMR (300 MHz, $CDCl_3$) δ ppm 7.95 – 7.88 (m, 4H), 7.87 – 7.76 (m, 5H), 7.57 – 7.43 (m, 2H), 7.36 – 7.29 (m, 2H), 2.40 (s, 3H).

H2 product is obtained using p-toluenesulfonyl hydrazide (1.51 g, 8.1 mmol) and 6-methoxy-2-naphthaldehyde (1.50g, 8.1 mmol) which leads to a white powder (2.56 g, 90 %).
^{1}H NMR (300 MHz, $CDCl_3$) δ ppm 10.11 (s, 1H), 8.10 (s, 1H), 7.92 – 7.76 (m, 6H), 7.40 (d, J = 8.1 Hz, 2H), 7.32 (d, J = 2.6 Hz, 1H), 7.17 (dd, J = 9.0, 2.6 Hz, 1H), 3.93 (s, 3H), 2.38 (s, 3H).

H3 product is obtained using p-toluenesulfonyl hydrazide (0.50 g, 2.6 mmol) and ethyl 6-formylnaphthalene-2-carboxylate (0.61g, 2.6 mmol) which leads to a white powder (0.67 g, 62 %). ^{1}H NMR (300 MHz, $CDCl_3$) δ ppm 10.34 (s, 1H), 8.61 (d, J = 1.5 Hz, 1H), 8.18 (s, 1H), 8.11 – 7.95 (m, 5H), 7.89 (d, J = 8.3 Hz, 2H), 7.41 (d, J = 8.1 Hz, 2H), 4.41 (q, J = 7.1 Hz, 2H), 2.38 (s, 3H), 1.41 (t, J = 7.1 Hz, 3H).

The diazonium salts **D1-3** have been synthesized using the following procedure: 1.5 ml of HCl (37 %) is added to a mixed solution of water / THF (15 ml / 10 ml) containing the appropriate naphthalene-based amine (1 eq. see the weights below). The solution is stirred during 30 min and cooled to -10 °C before addition of 1.4 eq. of $NaNO_2$. After 30 minutes stirring, 1.4 eq. of KPF_6 is added resulting to the appearance of a yellow precipitate. This precipitate is then filtered and successively washed with water, cold ethanol and cold ether. The diazonium salts are obtained after a final drying procedure under vacuum.

D1 product is obtained using 2-naphthylamine (0.70 g, 4.8 mmol), HCl 37% (1.5 ml), $NaNO_2$ (0.47g, 6.8 mmol) and KPF_6 (1.23g, 6.8 mmol) which leads to a yellow powder (1.15 g, 78 %). ^{1}H NMR (300 MHz, $CDCl_3$) δ ppm 9.73 (s, 1H), 8.63 – 8.53 (m, 2H), 8.42 (d, J = 8.3 Hz, 1H), 8.35 (d, J = 8.3 Hz, 1H), 8.19 – 8.11 (m, 1H), 8.05 – 7.98 (m, 1H).

D2 product is obtained using 6-methoxy-2-naphthylamine (0.52 g, 3.0 mmol), HCl 37% (1.2 ml), $NaNO_2$ (0.27 g, 3.9 mmol) and KPF_6 (0.72 g, 3.9 mmol) which leads to a yellow powder

(0.67 g, 68 %). ^{1}H NMR (300 MHz, $CDCl_3$) δ ppm 9.57 (d, *J* = 2.1 Hz, 1H), 8.50 (dd, *J* = 9.2, 2.2 Hz, 1H), 8.38 (d, *J* = 9.3 Hz, 1H), 8.34 (d, *J* = 9.3 Hz, 1H), 7.77 (d, *J* = 2.5 Hz, 1H), 7.60 (dd, *J* = 9.1, 2.5 Hz, 1H), 4.13 (s, 3H).

D3 product is obtained using ethyl 6-amino-2-naphthylcarboxylate (0.70 g, 3.2 mmol), HCl 37% (1.5 ml), $NaNO_2$ (0.31 g, 4.5 mmol) and KPF_6 (0.84 g, 4.5 mmol) which leads to a yellow powder (0.99 g, 81 %). ^{1}H NMR (300 MHz, $CDCl_3$) δ ppm 9.80 (d, *J* = 2.2 Hz, 1H), 8.96 (s, 1H), 8.78 (d, *J* = 9.1 Hz, 1H), 8.69 (dd, *J* = 9.1, 2.2 Hz, 1H), 8.54 (d, *J* = 8.7 Hz, 1H), 8.42 (dd, *J* = 8.7, 1.6 Hz, 1H), 4.49 (q, *J* = 7.1 Hz, 2H), 1.44 (t, *J* = 7.1 Hz, 3H).

The final step leading to the synthesis of the targeted tetrazoles can be described as follows: The p-toluenesulfonyl hydrazones **H1-3** (1 eq., see the weights below) were dissolved in 8 ml of pyridine and maintained at -20 °C. The diazonium salts **D1-3** (1 eq., see the weights below) dissolved in 15 ml of acetone are added dropwise during 20 min. The reactional mixture is then slowly warmed up to room temperature and stirred for 4 hours leading to the formation of a precipitate. After filtration, the precipitate is washed with cold acetone then dried under vacuum yielding the targeted tetrazole.

TCO was obtained with a yield of 29 % (0.58 g, white powder) using **H2** (0.2 g, 0.56 mmol) and **D1** (0.17g, 0.56 mmol).

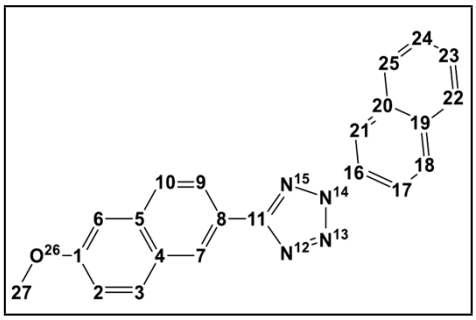

^{1}H NMR (500 MHz, CD2Cl2) δ ppm 8.75 (d, *J* = 1.7 Hz, 1H, [7]), 8.72 (d, *J* = 2.2 Hz, 1H, [21]), 8.37 (dd, *J* = 8.8, 2.1 Hz, 1H, [17]), 8.31 (dd, *J* = 8.5, 1.7 Hz, 1H, [9]), 8.10 (d, *J* = 8.8 Hz, 1H, [18]), 8.08 – 8.04 (m, 1H, [25]), 8.00 – 7.96 (m, 1H, [22]), 7.95 – 7.90 (m, 2H, [3], [10]), 7.69 – 7.68 (m, 2H, [23], [24]), 7.28 – 7.21 (m, 2H, [6], [2]), 9.96 (s, 3H, [27]). ^{13}C {^{1}H} NMR (126 MHz, CD_2Cl_2) δ ppm 165.9, [11], 159.3, [1], 136.3, [5], 134.8, [16], 133.8, [19], 133.6, [20], 130.6, [3], 130.4, [18], 129.1, [4], 129.0, [25], 128.4, [22], 128.0, [24], 128.0, [10], 127.8, [23], 127.1, [7], 124.9, [9], 122.8, [8], 120.1, [2], 118.6, [21], 118.3, [17], 106.3, [6], 55.8, [27]. HRMS (ASAP 160°C) m/z: $[M+H]^+$ Calculated for (C_{22} H_{17} N_4 O) T: 353.13969 Found: 353.1396 (0ppm).

TNO was obtained with a yield of 50 % (0.18 g, white powder) using **H1** (0.30 g, 0.92 mmol) and **D2** (0.31g, 0.92 mmol).

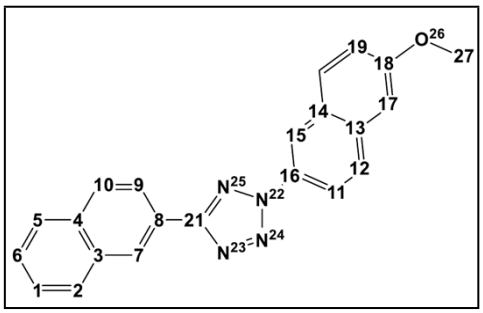

^{1}H NMR (500 MHz, CD2Cl2) δ ppm 8.83 (d, *J* = 1.7 Hz, 1H, [7]), 8.64 (d, *J* = 2.2 Hz, 1H, [15]), 8.35 (dd, *J* = 8.5, 1.7 Hz, 1H, [9]), 8.31 (dd, *J* = 8.9, 2.3 Hz, 1H [11]), 8.06 – 8.04 (m, 1H, [2]), 8.04 – 8.01 (m, 1H, [10]), 7.98 (d, *J* = 8.9 Hz, 1H, [12]), 7.96 – 7.94 (m, 1H, [20]), 7.94 – 7.92 (m, 1H, [5]), 7.62 – 7.55 (m, 2H, [1], [6]), 7.32 – 7.26 (m, 2H [19], [17]), 3.97 (s, 3H, [27]). ^{13}C {^{1}H} NMR (101 MHz, CD_2Cl_2) δ ppm 165.6, [21], 165.4, [18], 135.4, [13], 134.8, [4], 133.7, [3], 133.1, [16], 130.5, [20], 129.2, [2], 129.1, [10], 129.0, [12], 128.8, [14], 128.3, [5], 127.7, [1], 127.2, [6], 127.2, [7], 125.1, [8], 124.3, [9], 120.9, [19], 118.8, [11], 118.6, [15], 106.4, [17], 55.9, [27]. HRMS (ASAP 170°C) m/z: $[M+H]^+$ Calculated for (C_{22} H_{17} N_4 O): 353.13969 Found: 353.1401 (1ppm).

TCE was obtained with a yield of 48 % (0.14 g, white powder) using **H3** (0.3 g, 0.76 mmol) and **D1** (0.23g, 0.76 mmol).

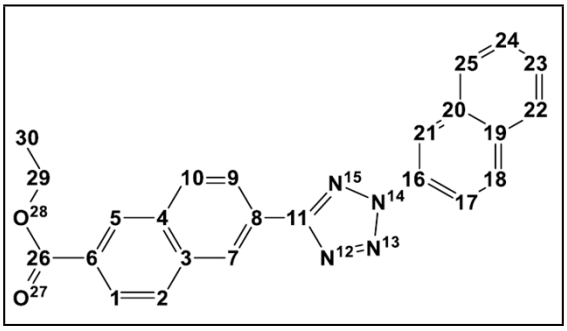

^{1}H NMR (500 MHz, CD_2Cl_2) δ ppm 8.83 (s, 1H, [7]), 8.68 (d, *J* = 2.4 Hz, 1H, [21]), 8.63 (s, 1H, [5]), 8.39 (dd, *J* = 8.5, 1.8 Hz, 1H, [9]), 8.33 (dd, *J* = 8.9, 2.3 Hz, 1H, [17]), 8.14 – 8.10 (m, 2H, [1], [10]), 8.07 (d, *J* = 8.9 Hz, 1H, [18]), 8.06 – 8.02 (m, 2H, [2], [25]), 7.99 – 7.94 (m, 1H, [22]), 7.66 – 7.59 (m, 2H, [24], [23]), 4.43 (q, *J* = 7.2 Hz, 2H, [29]), 1.45 (t, *J* = 7.2 Hz, 3H, [30]). ^{13}C {^{1}H} NMR (126 MHz, CD_2Cl_2): 166.6 [26], 165.3 [11], 135.7 [3], 134.6 [16], 133.9 [19], 133.9 [4], 133.5 [20], 131.0 [5], 130.6 [10], 130.4 [18], 129.5 [6], 129.3 [2], 129.0 [25], 128.4 [22], 128.0 [24], 127.9 [23], 127.1 [8], 126.9 [7], 126.5 [1], 125.0 [9], 118.6 [21], 118.2 [17], 61.7 [29], 14.6 [30]. HRMS (ASAP 170°C) m/z: $[M+H]^+$ Calculated for (C_{24} H_{19} N_4 O_2): 395.15025 Found: 395.1503 (0ppm).

TNE was obtained with a yield of 39 % (0.91 g, white powder) using **H1** (0.20 g, 0.62 mmol) and **D3** (0.23g, 0.62 mmol).

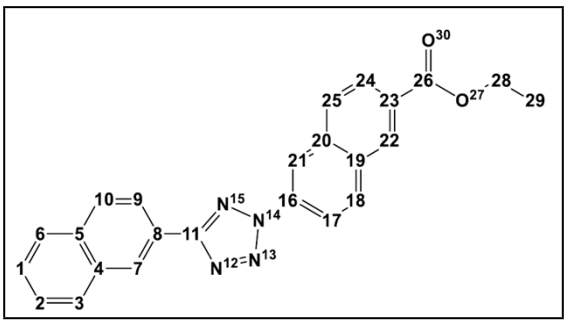

^{1}H NMR (500 MHz, CD_2Cl_2) δ ppm 8.84 (d, *J* = 1.7 Hz, 1H, [7]), 8.77 (d, *J* = 2.2 Hz, 1H, [21]), 8.70 (d, *J* = 1.6 Hz, 1H, [22]), 8.45 (dd, *J* = 8.9, 2.2 Hz, 1H, [17]), 8.35 (dd, *J* = 8.5, 1.7 Hz, 1H, [9]), 8.22 (d, *J* = 8.9 Hz, 1H, [18]), 8.19 (dd, *J* = 8.6, 1.7 Hz, 1H, [24]), 8.10 (d, *J* = 8.6 Hz, 1H, [25]), 8.06 – 8.02 (m,

2H, [3], [10]), 7.98 – 7.91 (m, 1H, [6]), 7.64 – 7.54 (m, 2H, [1], [2]), 4.45 (q, *J* = 7.1 Hz, 2H, [28]), 1.46z (t, *J* = 7.1 Hz, 3H, [29]).^{13}C {^{1}H} NMR (126 MHz, CD_2Cl_2) δ ppm 166.5 , [26], 165.9 , [11], 136.3 , [16], 135.7 , [20], 134.9 , [5], 133.7 ,[4], 133.0 , [19], 131.9 , [18], 131.0 , [22], 129.8 , [23], 129.3 , [25], 129.3 , [10], 129.1 , [3], 128.3 , [6], 127.8 , [1], 127.4 , [7], 127.3 , [2], 127.3 , [24], 124.8 , [8], 124.3 , [9], 119.0 , [17], 118.3 , [21], 61.8, [28], 14.6, [29]. HRMS (ASAP 170°C) m/z: $[M+H]^+$ Calculated for (C_{24} H_{19} N_4 O_2): 395.15025 Found: 395.1510 (2ppm).

3. Materials and General Characterization Methods.

Materials. All the solvents employed were Aldrich, Fluka or Merck spectroscopic grade. Pentaerythritol triacrylate (**PETIA**) monomer was purchased from Sartomer. Lucirin **TPO-L** was purchased from BASF (Ludwigshafen, Germany).

Steady-state absorption and fluorescence spectra. The absorption measurements were carried out with a JASCO V-730 spectrometer. Steady-state fluorescence spectra in solution were collected from a FluoroMax-4 spectrofluorometer. Emission spectra are spectrally corrected, and luminescence quantum yields include the correction due to solvent refractive index and were determined relative to quinine bisulfate in 0.05M (Φ_{fluo} = 0.52)[2].

Actinometry. The quantum yields for the tetrazole cycloreversion reactions were determined by irradiation of ACN solutions containing the tetrazole reactant (c = 0.15 mM) and **PETIA** (10 eq.) at $\lambda_{irr.}$ = 313 nm. All experiments were performed at 25°C in air equilibrated solutions which were continuously stirred. An Hg-Xe lamp (LC 9588/01A from Hamamatsu) equipped with a band pass filter centred at 313 nm (BP313-CWL from Edmund Optics) was used as irradiation source. The intensity of the incident light (8.4 x 10^{-7} einstein/min at 313 nm) was measured with the ferrioxalate actinometer[3]. The tetrazoles conversion rates which were monitored using reverse-phase HPLC (see **Figures S13-14**) are summarized in **Table S2**. **Figure S12** presents the plots for the time dependent generation of each pyrazoline.

	TCO	**TNO**	**TCE**	**TNE**
k_0 / $\mu M.s^{-1}$	1.6	5.7	4.6	4.2

Table S2. Values of tetrazoles conversion rates in ACN upon irradiation at 313 nm in presence of 10 eq. of PETIA (c = 0.15 mM for each tetrazole reactant)

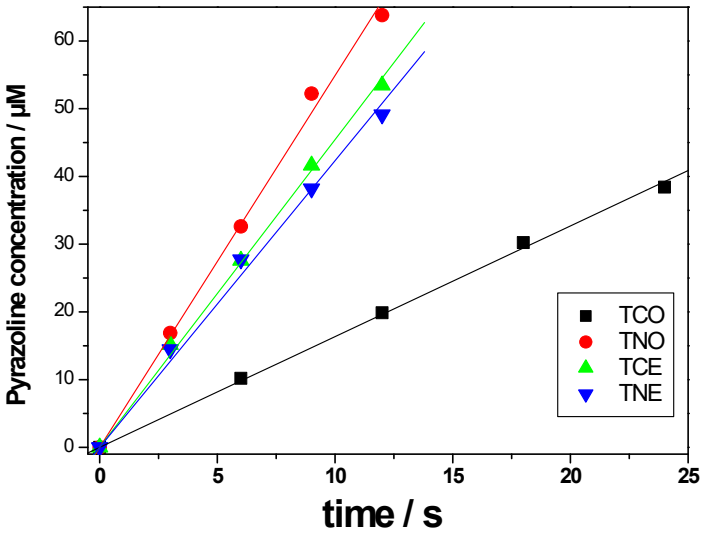

Figure S12. Time dependent generation of all pyrazoline cycloadducts during the actinometry photoclick experiments at 313 nm.

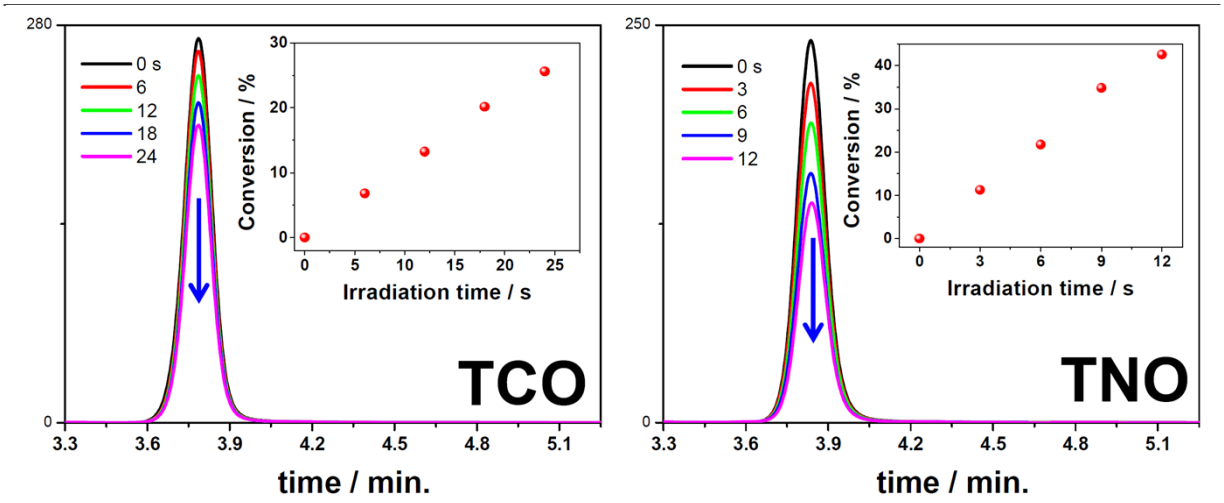

Figure S13. Evolution of the HPLC traces of **TCO** and **TNO** during irradiation at 313 nm in ACN in presence of **PETIA** co-reactant (10 eq.). Insets: Tetrazole conversion rate *vs.* irradiation time

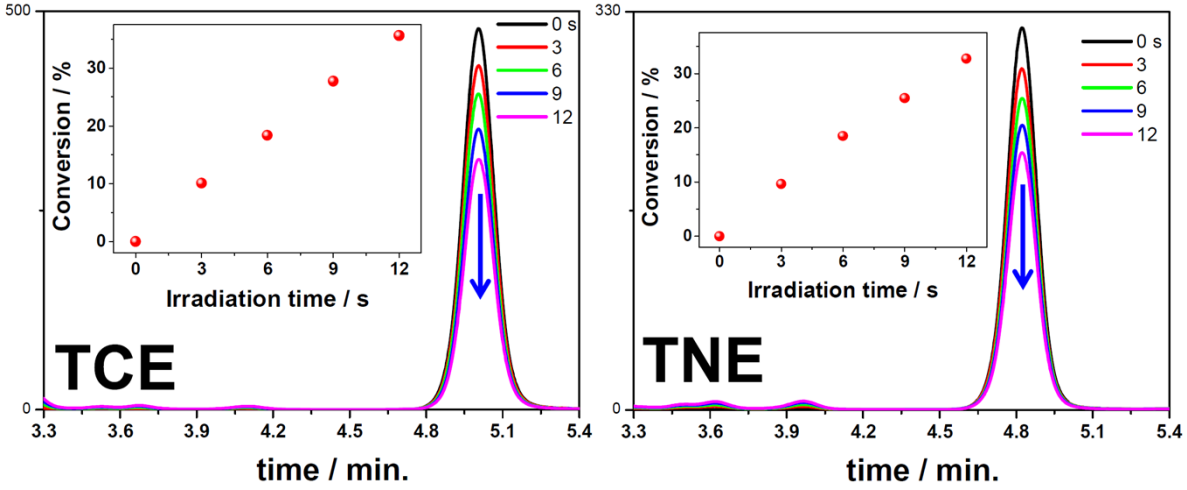

Figure S14. Evolution of the HPLC traces of **TCE** and **TNE** during irradiation at 313 nm in ACN in presence of **PETIA** co-reactant (10 eq.). Insets: Tetrazole conversion rate *vs.* irradiation time

---

Two-photon absorption spectra (2PA). The two-photon absorption (2PA) measurements were performed with femtosecond mode-locked laser pulse using a Ti: Sapphire laser (Spectra-Physics, Mai Tai: pulse duration: ~100 *fs*; repetition rate: 80 MHz; wavelength range: 690-1040 nm). Due to the sufficient emissivity of **TCO** (Φ_f = 0.21 in ACN), its 2PA spectrum was directly measured using the two-photon excitation fluorescence method[4-6] (2PEF). The measurements of 2PA cross-sections (δ) were performed relative to a reference molecule (*r*) : the 9,9-Didecyl- N^2,N^7-bis(4-methoxyphenyl)- N^2,N^7-diphenyl-9H-fluoren-2,7-diamine[7, 8] (**DAF**) in N,N-dimethylformamide. The value of δ for a sample (*s*) is given by:

$$\delta_S = \frac{S_S \Phi_r \eta_r c_r}{S_r \Phi_S \eta_S c_S} . \delta_r$$

Where *S* is the detected two-photon excited fluorescence integral area, *c* the concentration of the chromophores, and Φ is the fluorescence quantum yield of the chromophores. η is the collection efficiency of the experimental set-up and accounts for the wavelength dependence of the detectors and optics as well as the difference in refractive indices between the solvents in which the reference and sample compounds are dissolved. The measurements were conducted in a regime where the fluorescence signal showed a quadratic dependence on the intensity of the excitation beam, as expected for two-photon induced emission. For the calibration of the two-photon absorption spectra, the two-photon excited fluorescence signal of each compound was recorded at the same excitation wavelength as that used for the

standard. The laser intensity was in the range of 0.2-2 x 10^9 W/cm^2. The experimental error on the reported cross section is 15 %. **Figure S15** shows the 2PA spectrum of **TCO** in ACN which was superimposed with its corresponding 1PA one.

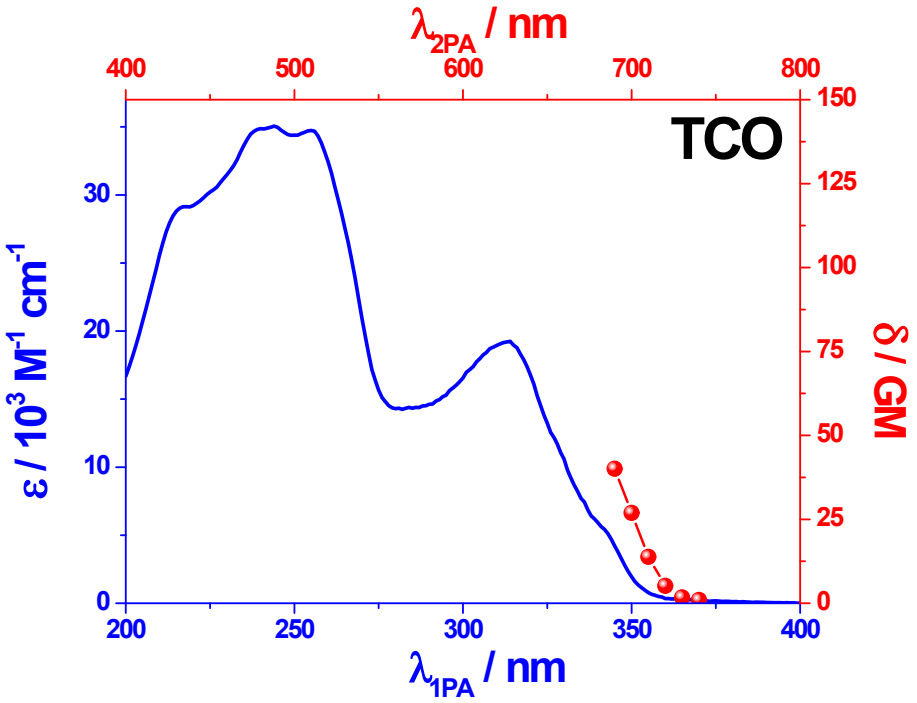

Figure S15. 1PA (blue line) and 2PA (red circles) spectra of **TCO** in ACN.

The 2PA spectra of the other tetrazoles have not been measured by 2PEF due to the low emissivity of the dyes (Φ_f < 0.1). As a consequence, their 2PA cross-sections have been measured by evaluating the consumption of tetrazole reactants during their respective 2P-induced cycloaddition reactions. For this purpose, isomolar ACN solutions of each tetrazole (c = 0.15M) were mixed with an excess of **PETIA** (10 eq.). Each solution was two photon irradiated at the same NIR wavelength during 30 min ($P_{irr.}$ = 700 mW). The total amount of two-photon converted tetrazoles has been evaluated using the pyrazolines fluorescence signals which were correlated to the conversion rate of the tetrazole reactants using HPLC technique. It should be noted that the tetrazole-ene reaction with **TCO** was used as a reference reaction since its 2PA cross-sections (δ^r_λ) have been already determined (see **Figure S15**). We also assumed that all the reaction quantum yields upon 2PA excitation are similar to those previously measured upon 1PA excitation. With this respect, the 2PA cross-sections (δ_λ) for each tetrazole can be derived using the following equations:

$$\frac{\Delta n}{\Delta n_r} = \frac{\delta_\lambda}{\delta_\lambda^r} \cdot \frac{c}{c_r} \cdot \frac{P^2}{P_r^2} \cdot \frac{\Phi}{\Phi_r}$$

In this equation Δn, c, Φ, P correspond respectively to the total amount of tetrazoles consumed during the 2P reactions, the concentration of the dye, the quantum yield of the photoreaction, the NIR laser irradiation power.

Two-Photon lithography. The 3D lithographic microfabrication was carried out using a Olympus IX73 inverted microscope. The two-photon microfabrication was performed at 800 nm using a mode-locked Ti: Sapphire oscillator (Spectra-Physics, Mai Tai: pulse duration: ~100 *fs*; repetition rate: 80 MHz; wavelength range: 690-1040 nm). The incident beam was focused through a 0.95 NA objective (40 X) which leads to a radial spot size 450 nm at λ_{exc} = 800 nm ($1/e^2$ Gaussian). A drop of the resin is deposited on a cover slip which is mounted on a 3D piezoelectric stage allowing the translation relative to the laser focal point. The intensity of the entering laser is controlled with the use of an acousto optic modulator. The displacement of the sample and all photonic parameters (i.e. excitation power and irradiation times) are computer-controlled. The 3D microstructure is finally obtained by washing away the unexposed monomer resin using ethanol.

Fluorescence labeling within polymer µ-structures upon two-photon excitation. The polyacrylate-based µ-slabs which were microfabricated have been functionalized with luminescence pyrazoline cycloadducts upon two-photon excitation. For this purpose, a home-made chamber composed with two distinctive PTFE pieces has been designed in order to sandwich the 18 x 18 mm glass coverslips containing the microstructures at their upper surface (see **Scheme S4**). Note that this PTFE cell is magnetically assembled using a sealing gasket leading to an inner volume of ~ 150 µl. The µ-slab can then be immersed in an ACN solution of tetrazole (c = 0.15 mM). The cell is then positioned on the same microscope used for microfabrication which allows two-photon excitation at the surface of the µ-slabs. The two-photon click functionalization was performing using a 20X, 0.40-NA objective at 700 nm with an input laser power of 1.3 mW and scanning speed of 100 µm/s . After the photoinduced labeling procedure, the glass coverslip is cleaned with chloroform than incubated in an ethanol bath to wash away the residual tetrazole reactants.

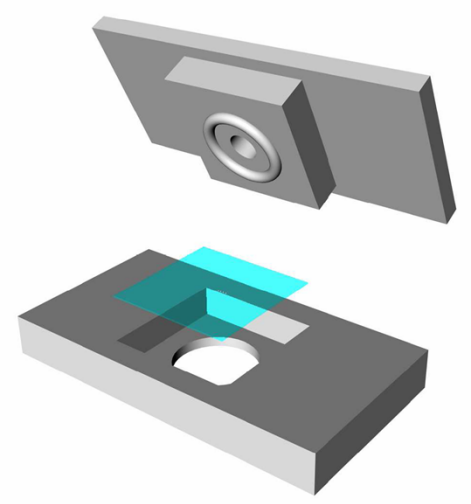

Scheme S4. Scheme of the PTFE chamber allowing immersion of µ-structures within ACN solutions containing tetrazole reactants and used for photoinduced labeling reactions.

Fluorescence microscopy. The time-dependent photoclick labeling of the µ-dots illustrated in **Figure 2C** has been performed by monitoring *in situ* the pyrazoline fluorescence signal using the same home-made cell which was positioned on an Olympus IX73 inverted microscope equipped with a 75 W Xe lamp housing. The microstructures immersed in ACN solution of tetrazole (c = 0.15mM) were continuously excited from the bottom of the chamber at $\lambda_{exc.}$ = 365 nm through a 40X, 0.65-NA objective using an Olympus U-FUN fluorescence mirror unit composed of a 365 nm band pass filter (BP360-370), a dichroic mirror (DM410) and long pass filter (BA420IF). The epifluorescence images were then recorded with a CMOS colour camera.

Chromatographic measurements. The progress of all the tetrazoles photoclick reactions during the 1PA or 2PA excitations was monitored using an HPLC JASCO liquid chromatography system (LC-4000 pump) coupled to UV and Fluorescence detections (UV4070 and FP4020 modules). An Innoval ODS-2 (C18, 4.6 x 15 mm, 5 µm particle size) column was used for the separation. The column was thermostated at 30 °C (±1 °C). The mobile phase consists in a 90:10 (v,v) mixture of ACN and milli-Q water. All the analyses were performed in isocratic mode with a flow rate of 1 mL/min.

4. References

1. N. Fournier-Le Ray, N. Joly and J.-L. Fillaut, *Tetrahedron*, 2023, **143**, 133560.
2. R. Meech and D. Phillips, *J. Photochem.*, 1983, **23**, 193–217.
3. M. Montalti, A. Credi, L. Prodi and M. T. Gandolfi, *Handbook of Photochemistry, Third Ed.*, CRC Press, Boca Raton, 2006.
4. C. Xu and W. W. Webb, *J. Opt. Soc. Am. B*, 1996, **13**, 481-491.
5. N. S. Makarov, M. Drobizhev and A. Rebane, *Opt. Express*, 2008, **16**, 4029-4047.
6. S. De Reguardati, J. Pahapill, A. Mikhailov, Y. Stepanenko and A. Rebane, *Opt. Express*, 2016, **24**, 9053-9066.
7. C. Martineau, R. Anémian, C. Andraud, I. Wang, M. Bouriau and P. L. Baldeck, *Chem. Phys. Lett.*, 2002, **362**, 291-295.
8. K. D. Belfield, M. V. Bondar, F. E. Hernandez, O. V. Przhonska and S. Yao, *J. Phys. Chem. B*, 2007, **111**, 12723-12729.